ARPN Journal of Engineering and Applied Sciences

www.arpnjournals.com

VEHICLE AERODYNAMICS ANALYSIS OF A MULTI PURPOSE VEHICLE USING CFD

Mohammad Firdaus Mohammed Azmi, Mohammad Al Bukhari Marzuki and Mohd Arzo Abu Bakar
Politeknik Sultan Azlan Shah, Behrang, Perak, Malaysia
E-Mail: firdaus_azmi@psas.edu.my

ABSTRACT

The aerodynamics analysis on a vehicle has become a major concern nowadays. This is due to its effect on vehicle driving characteristics, fuel consumption, etc. This study will analyse the aerodynamics characteristics of a multi-purpose vehicle (MPV) generic design using ANSYS Workbench. Fluent is utilised in this study in order to investigate the aerodynamics of generic MPV design, attaining coefficient of drag and lift and observing the airflow streamline across the body of the vehicle. The turbulence modelling selected is realizable k-ε with enhanced wall treatment. Based from the result obtained, the coefficient of drag and lift recorded for the car modelled is 0.28 and 0.05 respectively after the solution converged. This study can be used as reference for car manufacturers and designers especially when designing a multi-purpose vehicle (MPV) design.

Keywords: multi-purpose vehicle, ANSYS, fluent, aerodynamic analysis, k-e modelling.

INTRODUCTION

The aerodynamics characteristics of a vehicle directly affect the vehicle driving characteristics, stability, fuel consumption and safety features of the automobiles. The analysis of vehicles aerodynamics using computational method have been widely utilised by automobile manufacturer as the reference to their bodywork design in order to reduce drag and increase the down force for stability during manoeuvre.

The drag force acting on the vehicle is the consequence of vehicle surface in motion with stationary air in the surrounding. The sum of pressure differences mostly at the front and at the rear of the vehicle will result in the production of drag force. As the vehicle move forward, it will push the air to the side. This will increase the static pressure at the front of the vehicle. Meanwhile at the rear section of the vehicle, the air flow is unstable due to wake thus resulting in pressure drop. According to research by Juhala [6], the airflow surrounding a vehicle in motion is asymmetric with respect to its longitudinal axis. This is due to wind condition while driving and approaching traffic. The relative flow speed is the combination of driving speed and speed of wind.

In order to improve vehicle aerodynamics features, numbers consideration have been taken into account such as increasing the angle between the hood and the front windshield to get a better airflow around the car [3].According to Hucho [4], the size of separation at the windshield base is determined by the inclination angle between the bonnet and the windshield. When the inclination angle is larger, the air flowing outward to the A-pillar is smaller thus reducing the vortices produced. Another method proposed by [4] to reduce the value of coefficient of drag is by arching the roof in the longitudinal direction. This method somehow will change the frontal area thus increasing the drag force.

A research by Sneh [7] found that to get a good performance of a vehicle, it has to be aerodynamically efficient by reducing the drag force and increasing the down force for better handling. Next, [5] describe a favourable vehicle aerodynamics geometry as a vehicle which satisfy dynamics road behaviour by minimising airflow resistance and optimised aerodynamics lift.

A previous study has found that installation of a rear wing with an appropriate angle can reduce the aerodynamics lift coefficient [2]. It was found on the same study that the installation of an endplate can reduce the noise behind the car. It is clear that the vertical stability of a passenger car and its noise elimination can be improved. There are two types of separation described by [4] which is quasi-two-dimensional and three-dimensional. For quasi-two-dimensional separation, the governing equation is known as boat tailing. This parameter determined by the roof, side and undercarriage angles. The formation of three dimensional separations is determined by rear end angle. The objectives of boar tailing are to keep the area as small as possible.

The designs of the undercarriage also have been an attention recently. The car manufacturer aim is to keep the undercarriage to be as smooth as possible in order to eliminate the local vortices. [4] Suggested that application of small spoilers can be used in front of the component that produces local vortices. For example, tyre rotation will result in flow turbulence. The flow will spreads outwards and influencing yaw angle for flow contact with tyre.

This study will analyse the aerodynamics characteristics of a multi-purpose vehicle (MPV) generic design using ANSYS Workbench software package. ANSYS Fluent software is utilised in this study in order to investigate the aerodynamics of generic MPV design, measuring coefficient of drag and lift and observing the airflow streamline across the body of the vehicle.

METHODOLOGY

Governing equations

The governing equation for computational fluid dynamics solver are solely based on conservation of mass, momentum and energy. The continuity and momentum equation (Navier-Stokes) with a turbulence model were used to solve the airflow. The general form equation for the conservation of mass is written as

$$\frac{\partial P}{\partial t} + \nabla \cdot (\rho \vec{v}) = S_m \tag{1}$$

And can be used for both compressible and incompressible flow. S_m is the mass added to the continuous phase from the dispersed second phase due to vaporisation of liquid droplet.

Turbulence modelling

The turbulence modelling selected for this study is realizable k-ε with enhanced wall treatment. The reason is that this turbulent modelling contains new formulation for turbulence viscosity and it has new transport equation for the dissipation rate, ε have been derived from exact equation for the transport of the mean square vorticity fluctuation. The advantages of using this turbulence model is that it able to accurately predicts the spreading of both planar and round jets. Furthermore, it also able to provide greater performance for flow involving rotation, boundary layers under strong adverse pressure gradients, separation and recirculation (ANSYS, 2009)

The mathematics behind the realizable k-ε is the combination between Boussinesq relations with eddy viscosity equation.

Transport equation for realizable k-ε model

For turbulence kinetic energy(k)

$$\frac{\partial}{\partial t}(\rho k) + \frac{\partial}{\partial x_j}(\rho k u_j) = \frac{\partial}{\partial x_j}\left[\left(\mu + \frac{\mu_t}{\sigma_k}\right)\frac{\partial k}{\partial x_j}\right] + G_k + G_b - \rho\epsilon - Y_M + S_k \tag{2}$$

And for dissipation (ϵ)

$$\frac{\partial}{\partial t}(\rho \epsilon) + \frac{\partial}{\partial x_j}(\rho \epsilon u_j) = \frac{\partial}{\partial x_j}\left[\left(\mu + \frac{\mu_t}{\sigma_k}\right)\frac{\partial \epsilon}{\partial x_j}\right] + \rho C_1 S_\epsilon - \rho C_2 \frac{\epsilon^2}{k + \sqrt{v\epsilon}} + C_{1\epsilon}\frac{\epsilon}{k} C_{3\epsilon} G_b + S_\epsilon \tag{3}$$

Where

$$C_1 = max\left[0.43, \frac{\eta}{\eta + 5}\right], \qquad \eta = S\frac{k}{\epsilon}, \qquad S = \sqrt{2S_{ij}S_{ij}}$$

From the equations, G_k characterises the turbulence kinetic energy due to the mean velocity gradients and G_b characterises generation of turbulence kinetic energy as the effect of buoyancy. Y_M signifies the influence of the fluctuating dilatation in compressible turbulence to the total dissipation rate. Next, C_{1e}, C_{2e} and C_{3e} are constants. σ_k and σ_e are the turbulent Prandtl numbers for k and ε, respectively. Lastly, S_k and S_e are source terms defined by user (ANSYS, 2009).

Turbulence viscosity modelling

To compare between the realizable k-ε modelling and standard k-ε models is that C_μ is not constant. It can be computed from

$$C_\mu = \frac{1}{A_0 + A_s \frac{kU^*}{\epsilon}}$$

Where

$$U^* \equiv \sqrt{S_{ij}S_{ij} + \tilde{\Omega}_{ij}\tilde{\Omega}_{ij}}$$

And

$$\tilde{\Omega}_{ij} = \Omega_{ij} - 2\epsilon_{ijk}\omega_k$$
$$\Omega_{ij} = \overline{\Omega_{ij}} - \epsilon_{ijk}\omega_k \tag{4}$$

Where $\overline{\Omega_{ij}}$ is the rate of rotation tensor, viewed in a rotating reference frame with the angular velocity ω_k. The model constants A_0 and A_s are:

$$A_0 = 4.04, \qquad A_s = \sqrt{6}\cos\phi$$

Where,

$$\phi = \frac{1}{3}\cos^{-1}\left(\sqrt{6}W\right),\ W = \frac{S_{ij}S_{jk}S_{ki}}{\tilde{S}^3}, S = \sqrt{2S_{ij}S_{ij}}, \quad S_{ij} = \frac{1}{2}\left(\frac{\partial u_j}{\partial x_i} + \frac{\partial u_i}{\partial x_j}\right) \tag{5}$$

Model constants

C_μ is a function of the mean strain and rotation rates, the angular velocity of the system rotation and the turbulence field (k and ϵ).

The model constants C_2, σ_k and σ_ϵ have been established to ensure that the model performs well for certain canonical flows. The model constants are

$$C_{1e} = 1.44, \quad C_2 = 1.9, \quad \sigma_k = 1.0, \quad \sigma_c = 1.2$$

COMPUTATIONAL DOMAIN AND BOUNDARY CONDITIONS

Modelling of a generic MPV design

The car model was designed using CATIA V5 software package. The body mostly created using Generative Shape Design module. The basic design of the vehicle are based on blueprint of a PROTON Exora and some modification have been made however some modification have to been made to differentiate the model into general design of an MPV. The design have been simplified by removing some components such as exhaust system, braking system, side mirror and other small component to reduce computational cost. Figure-1 and

VOL. 12, NO. 7, APRIL 2017 ISSN 1819-6608
ARPN Journal of Engineering and Applied Sciences

Figure-2 shows the isometric front and isometric back rendered model of the MPV respectively.

Figure-1. Rendered isometric front view.

Figure-2. Rendered isometric back view.

Meshing

The computational domain is defined as the half body to reduce computational cost. This is valid because a vehicle has symmetry in vertical plane along its longitudinal axis. For this study, only triangular meshing is applied because of the complexity of geometry of the vehicle. The number of node produced from the meshing process are 207619 with 1181813 tetrahedral cell. Figure-3 shows the meshing elements and mesh density on the model. The mesh made denser especially around the car to obtain more accurate result.

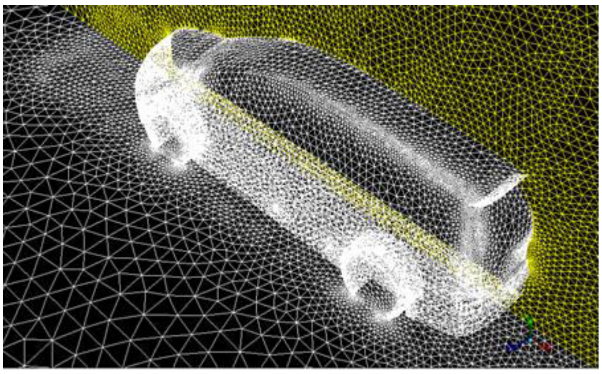

Figure-3. Tetrahedral meshing of the model.

Boundary conditions

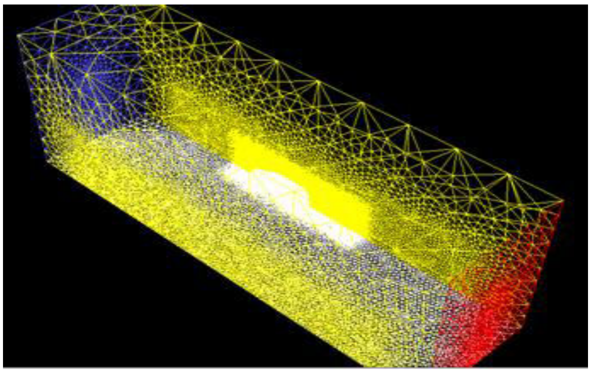

Figure-4. Overall meshing and boundary conditions.

The domain around the body is considered as the actual size of the wind tunnel. Wall of the wind tunnel, side and top faces of the domain are assumed to be symmetry. Figure-4 shows the overall grid generation and the boundary conditions of the model.

The inlet velocity (blue face) is specified at 55.55m/s (≈200km/h) based from the maximum speed of the vehicle according to manufacturer specification. The turbulence intensity and the turbulent viscosity ratio is set at 1% and 10 respectively. While at the outlet (red face), backflow turbulence intensity is specified at 5% and backflow turbulent viscosity ratio is constant at 10.

The boundary conditions are defined as velocity inlet, pressure outlet, symmetry and stationary wall. The wall of the wind tunnel (side, top face) is defined as symmetry and coloured yellow in Fluent. Next, the white surface represent a stationary wall in which for this study are the car body and the road surface. The boundary conditions can be simplified as Table-1 below:

Table-1. Overall boundary conditions.

Boundary	Boundary types	Values
Inlet	Velocity_inlet	55.55m/s
Outlet	Pressure_outlet	0 gauge pressure
Top	Symmetry	-
Side	Symmetry	-
Bottom	Stationary wall	-
Car Body	Stationary wall	-

From model designed from computer aided design (CAD) software the projection area calculated as the reference value is $1.45m^2$ and the air is assumed to be an ideal gas for this study.

RESULT AND DISCUSSIONS

Computational analysis of a multi-purpose vehicle design was carried out using ANSYS Fluent to investigate the air flow around the vehicle body, the coefficient of drag and lift. The car is assumed to be moving at 200km/h.As the analysis run converged, the result extracted from the software are to be discussed.

Coefficient of drag and lift

Coefficient of drag is dependable on the design of the body. Based from the result obtained, the coefficient of drag recorded for the car modelled is 0.28 after the solution converged. Figure-5shows the graph of coefficient of drag vs. number of iteration.

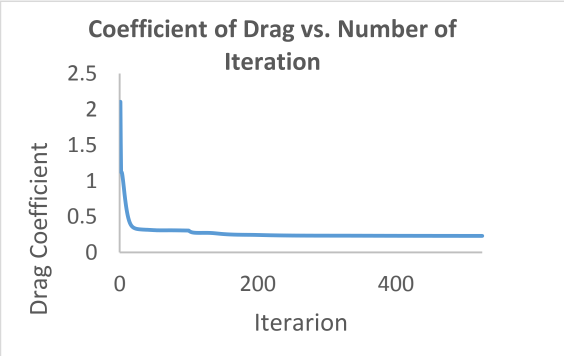

Figure-5. C_d vs. number of iteration.

Table-2. MPV coefficient of drag from manufacturer specification.

Model	Year	Cd
Vauxhall Zafira Tourer	2011	0.28
Peugeot 5008	2009	0.29
Volkswagen Touran	2015	0.296
Honda Odyssey	2005	0.3
Toyota Sienna	2003-2009	0.3
Honda Stream	2004	0.3
Ford S-Max	2011	0.3
Mazda MPV	2004	0.34
Toyota Previa	1991-1997	0.35

Table-2 shows the comparison of drag coefficient for various MPV class automobile models based from its manufacturer specification. It can be found from the table that for average MPV design, the coefficient of drag recorded is 0.3. The results obtained from this analysis are comparable to the average of most MPV coefficient of drag value and level to Vauxhall Zafira Tourer which recorded the lowest Cd among most MPV segment. The result of this analysis for coefficient of drag cannot be compared to original body shape blueprint PROTON Exora since PROTON does not announce the drag coefficient of Exora model to public.

Meanwhile, the coefficient of lift recorded for this analysis is 0.05 as inFigure-6. The value of lift coefficient illustrate the value of the down force acted on the vehicle. Negative lift is very useful in achieving cornering stability and mostly required for racing vehicle. However, as the down force increase, it can lead to higher drag values recorded as the drawback. Nowadays, most supercars are equipped with active rear spoiler which can flap according to driving conditions. The rear spoiler optimises the airflow at the back of the vehicle and during heavy braking, it can tilt almost vertical to increase drag and down force for better grip on road.

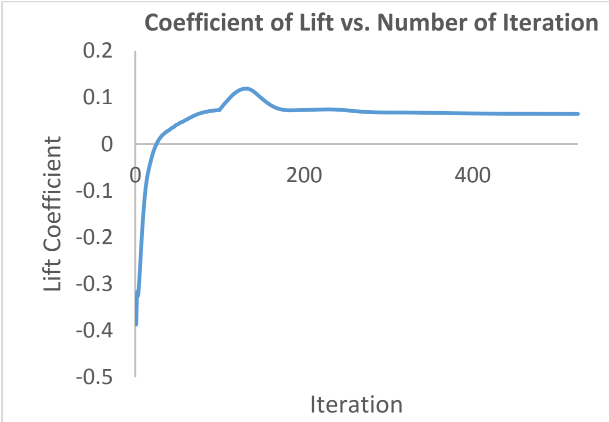

Figure-6. C_l vs. number of iteration.

Velocity vector and velocity streamline

Figure-7 show the vector of velocity magnitude of the MPV. It obvious to see that the air velocity is decreasing as it approach the front section of the car (blue arrow). Then air velocity increases away from the car front to the A-pillar. The red arrow indicates the highest airflow velocity and can be spotted at the front side (A-pillar) of the car and the back side (C-pillar) of the car. The maximum airflow velocities recorded are 87.2 m/s located at the A-pillar section. The air accelerated from vehicle front area to the A-pillar is because of the difference of pressure. High pressure recorded when the air stagnatesat the front area of the vehicle and it moves towards lower pressure area which is at the A-pillar.

Velocity contour on the symmetry plane are extracted from the analysis result as in Figure-8. The maximum velocity magnitude recorded at the symmetry plane is 78.6m/s which are at the area of the vehicle A-pillar. As we can observe from the velocity magnitude plot, as the car moving at constant speed of 55.55m/s, the blue region in the contour plot shows the lowest airflow velocity of the system. The lowest airflow velocity can be found the rear of the vehicle.

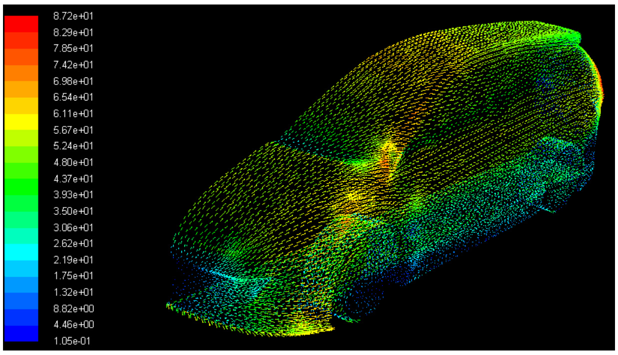

Figure-7. Vector of velocity magnitude.

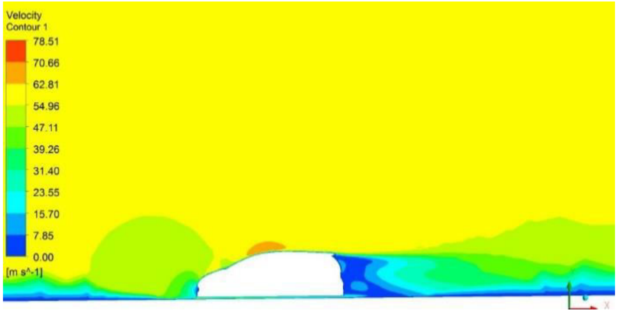

Figure-8. Velocity contour on symmetry plane.

Static pressure

Results of static pressure contours are combined with the velocity streamline as in Figure-9.

It is obvious from the Figures-9 that there is a higher pressure concentration on the car at the front section. The airflow will slow down when it approaches the front area of the vehicle and will result in the air accumulated into a smaller space. Once the air stagnates at the frontal area of the car, it will flow to lower pressure area such as the hood and roof, sides and bottom of the car.

When the air flows over the vehicle hood, the pressure decreasing. However, when it reaches the windscreen, the pressure increases. When the higher-pressure air in front of the windshield travels over the windshield, it accelerates, causing the decrease of the pressure. This lower pressure literally produces a lift -force on the car roof as the air passes over it (Darko Damjanović & Živić, 2010). Maximum pressure recorded is 1.892kPa at the region where the air stagnates while the minimum is -3.51kPa.The pressure contour distribution on symmetry plane can be seen as inFigure-10.

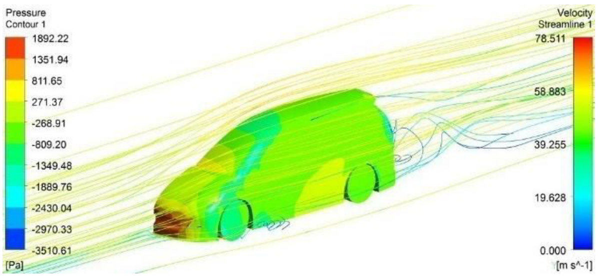

Figure-9. Pressure contour and velocity streamline

Figure-10. Pressure contour on symmetry plane.

Turbulence kinetics energy

Figure-11 shows the turbulence intensities streamline for back view of the vehicle. As we can analyse from the result, there are two areas where high turbulence can be spotted which are at the front wheel bay area and at the rear of the vehicle. However, the result is less accurate since this study does not includes the rotating wheel in the analysis. The maximum of the turbulence intensities of the vehicle is 24.1Jkg^{-1} found at the rear wing of the vehicle.

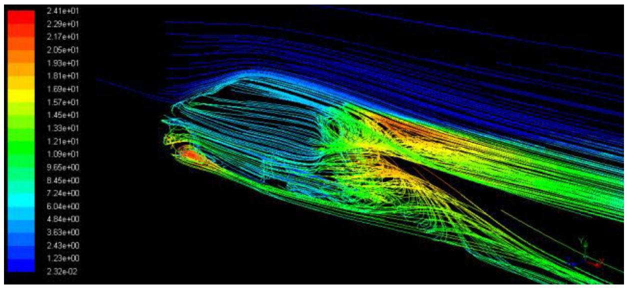

Figure-11. Turbulence intensities streamline (back).

Figure-12 shows the contour of turbulence kinetic energy on the symmetry plane. As we can observed, the maximum value of turbulence kinetic energy was found at the rear section of the vehicle after flow separation at the rear wings.

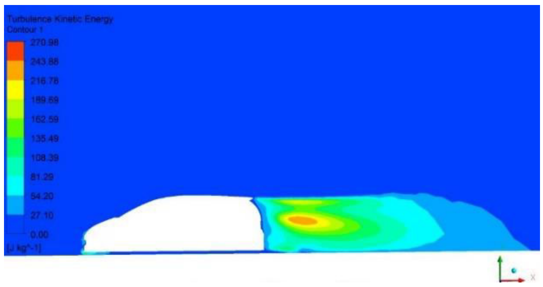

Figure-12. Contour of turbulence kinetic energy on symmetry plane.

CONCLUSIONS

A three dimensional computational fluid dynamics analysis was carried out using ANSYS Fluent on a generic multi-purpose vehicle body design to analyse the aerodynamics characteristics of the body shape of the vehicle in that segment. Based from the result found that the body design of the MPV segment will produce coefficient of drag between 0.28 to 0.35 and coefficient of lift of 0.05. While based on the velocity streamline and turbulence kinetic energy results, it can be concluded that the rear section of the vehicle still need to be improve since the turbulence energy detected develop because the high speed air from the roof of the vehicle stagnates with the lower velocity of air from the back of the vehicles. This study also can be used as reference for car manufacturers especially for designing a multi-purpose vehicle (MPV) design.

FUTURE WORKS

For future studies, we would like to analyse the vehicle aerodynamics in more details such as rotating wheels and air flow under the bonnet and cabin. The result will be more accurate since it already taken account of all details of the vehicle. However, this process will cost us a lot of time and computational power especially when modelling the car interior and engine. The computational time and cost to run the simulation on ANSYS also will increase dramatically.

REFERENCES

[1] ANSYS. 2009. ANSYS FLUENT 12.0 Theory Guide.

[2] Chien H. T. 2009. Computational aero-acoustic analysis of a passenger car with a rear spoiler. Applied Mathematical Modelling. 33 (9): 3661-3673.

[3] Darko D. D. K. and Živić M. 2010. CFD analysis of concept car in order to improve aerodynamics. International Scientific and Expert Conference TEAM.

[4] Hucho W. 1998. Aerodynamics of Road Vehicles. SAE.

[5] Hünergarth S. A. 2011. Audi Q3 aerodynamics and aeroacoustics. ATZ Extra.

[6] Juhala M. 2014. Improving vehicle rolling resistance and aerodynamics. Woodhead Publishing Limited.

[7] Sneh H. M. G. 2014. Aerodynamic Study of Formula SAE Car. Procedia Engineering. 97: 1198-1207.